# High-Temperature Behavior of Polyethylene-Terephthalate- Fiber-Reinforced Sand Concrete: Experimental Investigation

**Benzerara, M., Biskri, Y., Saidani, M., Slimani, F. & Belouettar, R**

# High-Temperature Behavior of Polyethylene-Terephthalate-Fiber-Reinforced Sand Concrete: Experimental Investigation

**Mohammed Benzerara** [1,*]**, Yasmina Biskri** [2]**, Messaoud Saidani** [3,*]**, Fayçal Slimani** [4] **and Redjem Belouettar** [4]

1 Materials, Geomaterials and Environment Laboratory (LMGE), Faculty of Technology, Department of Civil Engineering, Badji Mokhtar-Annaba University, P.O. Box 12, Annaba 23000, Algeria

2 Laboratory of Anticorrosion-Materials, Environmental and Structure LAMES, Higher Normal School of Technological Education, University of 20 août 1955 Skikda, Skikda 21000, Algeria; biskriyasmina@yahoo.fr

3 Research Institute of Clean Growth and Future Mobility, Coventry University, Priory Street, Coventry CV1 5FB, UK

4 Civil Engineering Laboratory (LGC), Faculty of Technology, Department of Civil Engineering, Badji Mokhtar-Annaba University, P.O. Box 12, Annaba 23000, Algeria; slimani_faycal@yahoo.fr (F.S.); redjem.belouettar@univ-annaba.dz (R.B.)

* Correspondence: mohammed.benzerara@univ-annaba.dz (M.B.); m.saidani@coventry.ac.uk (M.S.)

**Abstract:** At ambient temperature, concrete exhibits excellent mechanical properties. However, understanding the behavior of concrete under high-temperature conditions is crucial, especially for civil engineering applications during fire incidents. The growing use of plastic-based products has led to a significant increase in polymer waste, posing environmental challenges. The valorization of this plastic waste in the form of fibers presents both economic and environmental advantages. This study focuses on the study of the behavior of sand concrete incorporating polyethylene terephthalate (PET) fibers with percentages of 1% and 2% at high temperatures (100, 300, 500 and 700 °C). Specimens are tested for residual mass loss, residual compressive and tensile strength. A complementary analysis of SEM makes it possible to confirm and better clarify the morphology of the concretes of sand before and after the rise in temperature. The results obtained from this study indicate that the residual resistance is reduced with the rise in temperature for all the concretes studied, except in the temperature range of 300 °C, in which a slight improvement in resistance is noticed. The incorporation of PET fibers in the test concretes does not enhance their residual behavior significantly. However, it does serve as an effective solution by reducing the susceptibility to spalling, by preventing cracking and by fulfilling a similar role to that of polypropylene fibers.

**Keywords:** sand concrete; PET fibers; high temperature; mass loss; mechanical resistance

## 1. Introduction

Over the past 100 years, concrete has revolutionized the world's built environment. Around the world, concrete structures have become essential to houses in an ever-growing population. Global concrete production in 2020 was 14.0 billion $m^3$ and is still progressing over time according to Global Cement and Concrete Association, making it the most widely used manufactured material in the world [1]. This material is used in the construction of residential buildings, tunnels, industrial and commercial buildings, engineering structures, etc. Concrete is a suitable material as it remains strong and durable for a long time. However, in extreme situations, such as a fire, concrete can be damaged to varying degrees [2–4]. There are many examples of structures, including tunnels, that suffered from fires: Windsor Tower, Madrid, 2005; Channel Tunnel, 1996–2008; Mont Blanc Tunnel, 1999; Gotthard tunnel, 2001; Howard Street Tunnel, 2001; Frejus Tunnel, 2005; and fires in Algeria in the Kabylia region, 2021 [5,6].

Fires in concrete structures have highlighted the impact of high temperatures on concrete damage [2,3]. Buildings must meet several safety criteria to protect people, the

structure and the environment in the event of a fire. Due to the formulation of concrete, the phenomena that occur during fires are complex [7].

The effects of high temperatures on the properties of concrete have been reported. Concrete can become thermally unstable above a certain temperature and steadily degrades from the outside to the core throughout the heating process, leading to delamination of the material, loss of mechanical strength and even deactivation of the framework [2].

The fire behavior of ordinary Portland concrete is influenced by both thermal and chemical factors. When exposed to temperatures above 400 °C, stresses are generated due to the different coefficients of expansion of cement paste and aggregates. As the aggregates expand, the cementitious matrix undergoes thermal shrinkage, leading to the formation of microcracks near the cement–aggregate interface. From a chemical point of view, the thermal changes that occur in Portland concrete during a fire involve the evaporation of free water (occurring at around 100 °C), the decomposition of the CH phase (occurring at above 350 °C) and degradation of CSH hydrate gel (occurring above 500 °C). These transformations cause an increase in the porosity of the concrete and a decrease in its strength. Therefore, Portland concrete becomes structurally unsuitable at temperatures exceeding 600 °C. Thus, research efforts have been devoted to exploring the use of geomaterials in concrete to promote innovation by allowing the development of concretes resistant to high temperatures [8].

The behavior of concrete at high temperature varies according to its composition and its initial properties. One of the solutions to spalling is the incorporation of fibers into the concrete such as synthetic fibers of polypropylene [9–11]. Adding polypropylene fibers to concrete improves its thermal stability. They melt and evaporate, generating a channel that facilitates the transport of water flows. The study of concretes containing fibers shows, in the presence of polypropylene, a decrease in the vapor pressure peak with the rise in temperature. This decrease is related to the volume of fibers [12–15]. The study of the influence of metal fibers on the behavior of concrete brought to high temperature shows for some authors a thermal instability at low temperature (below 200 °C) or delayed instability (from 800 °C) [16,17]. Several parameters may be at the origin of the observed differences: the mode of hardening of the specimens (dry or saturated specimens); the heating rate; and the fiber content, which seems to be a preponderant factor [18]. The high quantity of fibers can also generate an additional thermal gradient, which would lead to the phenomenon of thermal instability [12,14].

In recent years, several researchers have studied the effects of different plastic wastes on the properties of concrete [19]. Some of the most common waste plastics used for concrete reinforcement include waste polyethylene terephthalate (PET) bottles [20–22], waste polyethylene (PE) bags [23], polyvinyl alcohol fibers (PVA) [24] and waste polypropylene fibers (PP) [25]. This plastic waste is likely to be used as a fibrous material in the production of durable concrete to prevent micro-cracking and to improve the durability of concrete [8,20].

Kim S.B et al. demonstrated that the results reveal that the addition of PET fibers improves the ductility and toughness of concrete, helping to improve crack resistance and post-crack behavior. Additionally, durability tests indicate that RPET-FRC exhibits satisfactory resistance to water absorption, freeze–thaw cycles and chloride penetration, ensuring long-term durability [20]. Foti D found that using PET fibers from waste bottles as reinforcement in concrete shows promise for improving the performance of the material and provides a sustainable and cost-effective alternative in construction [21]. Al-Hadithi A.I et al. concluded that the incorporation of waste plastic fibers improves the fresh properties by increasing the viscosity and stability of the concrete mix and alleviates the drying shrinkage of self-consolidating concrete [23]. Mohammadhosseini H and Yatim J.M concluded that the addition of carpet waste fibers and POFA influences the microstructure of concrete. The incorporation of these materials leads to a more refined microstructure with reduced pore size and improved interfacial bonding between the matrix, and the

fibers exhibit better resistance to thermal degradation and improved post-fire performance compared with ordinary concrete [25].

The main objective of this study is to explore the valorization of plastic waste, specifically PET fibers, in the formulation of high-temperature-resistant sand concrete. The study aims to investigate the potential of PET fibers as an alternative to the commonly used polypropylene fibers in this context. PET fibers are available in large quantities in Algeria, replacing polypropylene fibers, which are expensive fibers. It may offer advantages such as ease of processing and low cost over other fibers. PET fibers are lightweight, are easy to handle and can be mixed with concrete without disturbing the casting process. They are recyclable and inexpensive and can provide environmental benefits by reducing the amount of plastic waste that ends up in landfills. These fibers have low thermal conductivity and low density, which can reduce the spread of heat through concrete and can help prevent cracking and premature failure of concrete when exposed to high temperatures. PET fibers can also help maintain the structural integrity of concrete by improving ductility and flexural strength, as well as by reducing the formation of cracks due to thermal contraction upon cooling. This can extend the life of concrete and reduce long-term maintenance costs. In the context of sustainable development, it is important to mention that, in this study, granulated slag geomaterials sourced from the blast furnace of El-Hadjar (Annaba, Algeria) were incorporated as filler into the formulation of sand concrete. The purpose was to enhance specific physical–mechanical properties of the concrete.

## 2. Experimental Approach

### 2.1. Cement

The cement used is of the type CEM I 42.5/A according to the European standard EN 197-1 [26], supplied by the company of Biskra (Algeria). The different chemical composition and physical properties of the cement are given in Tables 1 and 2.

**Table 1.** Chemical composition of cement CPA-CEM I 42.5.

| Element | CaO | $Al_2O_3$ | $Fe_2O_3$ | $SiO_2$ | MgO | $Na_2O$ | $K_2O$ | $Cl^-$ | CaO Free | Loss of Fire |
|---|---|---|---|---|---|---|---|---|---|---|
| Percentage (%) | 64.18 | 5.18 | 3.74 | 22.27 | 0.70 | 0.2 | 0.44 | 0.19 | 0.6 | 1.35 |

**Table 2.** Physical characteristics of cement CPA-CEM I 42.5.

| Setting Time TD | | Normal Consistency | Apparent Density ($g/cm^3$) | Absolute Density ($g/cm^3$) | Specific Surface (BLAINE) |
|---|---|---|---|---|---|
| Beginning $T_i$ | End $T_f$ | 29 | 1.05 | 3.0 | 3070 |
| 2 h 28 min | 4 h 10 min | | | | |

### 2.2. Filler

In the current study, granulated slag filler according to the European standard NF EN 15167-1 [27] was used.

Tables 3 and 4 show the different chemical compositions and physical properties of the granulated slag filler.

**Table 3.** Chemical composition of granulated slag.

| CaO | $SiO_2$ | $Al_2O_3$ | $Fe_2O_3$ | MgO | $K_2O$ | $Na_2O$ | $SO_3$ | $Cl^-$ | P.A.F |
|---|---|---|---|---|---|---|---|---|---|
| 39.2 | 38.9 | 8.98 | 0.85 | 9.59 | 0.89 | 0.10 | 0.07 | 0.01 | - |

**Table 4.** Physical characteristics of granulated slag.

| Absolute Density (g/cm$^3$) | Apparent Density (g/cm$^3$) | Specific Surface (BLAINE) |
|:---:|:---:|:---:|
| 2.88 | 1.03 | 3640 |

## 2.3. Aggregates

Two types of sand were used in this study, a fine siliceous sand 0/2 and a crushed limestone sand 1.25/5. Table 5 shows the physical properties of the sands used, and Figure 1 shows the granulometric curve.

**Table 5.** Physical properties of sands.

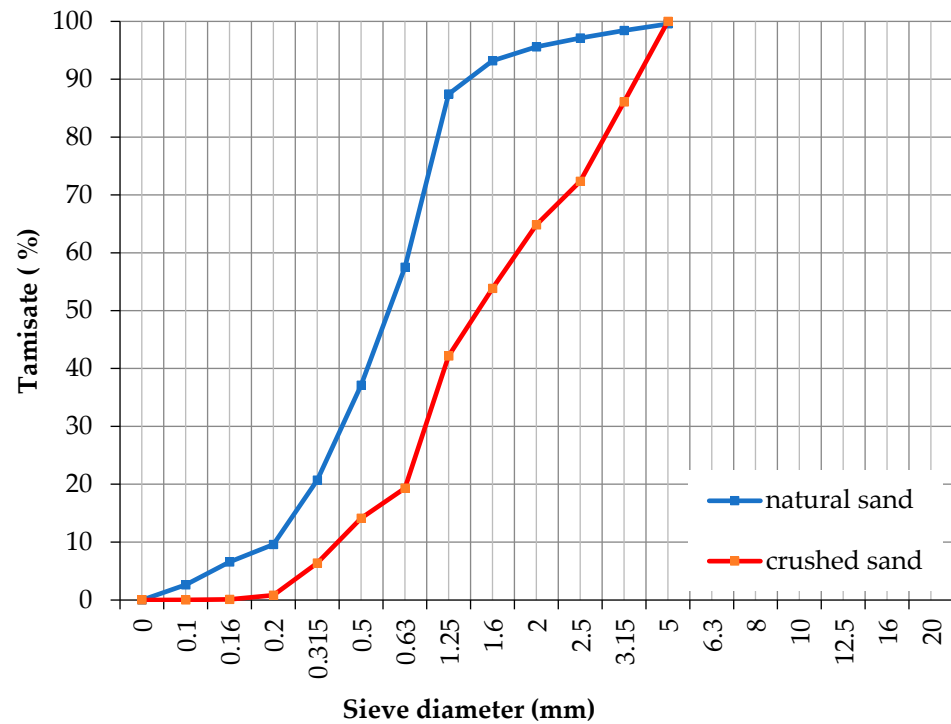| Characteristics | Unit | Dune Sand | Quarry Sand |
|:---|:---:|:---:|:---:|
| Finesse module | - | 2.10 | 3.45 |
| Apparent density | g/cm$^3$ | 1.65 | 1.46 |
| Absolute density | g/cm$^3$ | 2.60 | 2.65 |
| Cleanliness (ES) | % | 63.46 | 55.03 |



**Figure 1.** Size analysis of the different sands used.

## 2.4. PET Fibers

PET fibers supplied by the company **RET-PLAST** were used, located in the region of Mezloug-Sétif (Algeria), which specializes in the recycling of post-consumer PET bottles in the form of polyester fibers (Figure 2).
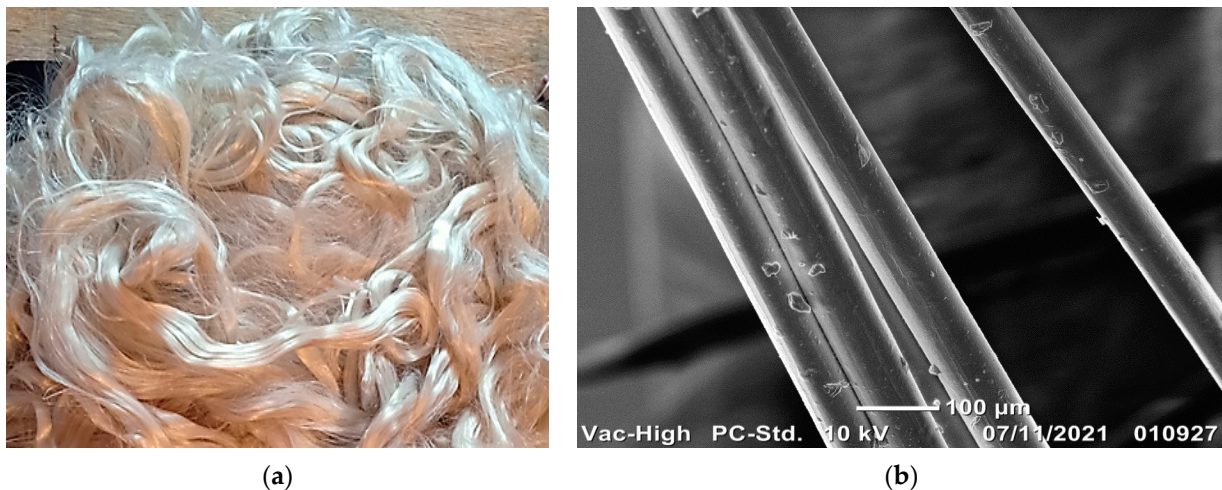
(**a**)

(**b**)

**Figure 2.** (**a**) Optical picture of PET fibers; (**b**) SEM picture of PET fibers.

The characterization of the PET fiber at the **Mediterranean Wires (MediFil)** company (Setif, Algeria) gave us the physical and mechanical properties summarized in Table 6 [28].

**Table 6.** Physical and mechanical properties of PET fiber [28].

| Properties | Values |
| --- | --- |
| Density at 20 °C | 1.16 |
| Cutting length (mm) | 70.00 |
| Metric Number (Nm) | 557.00 |
| Title (DTex) | 18.00 |
| Size (Denier) | 16.16 |
| Pressley Index (lb/mg) | 6.97 |
| Pressley (Pound/Pouc$^2$) | 73.00 |
| Breaking length (gf/Tex) | 37.39 |
| Relative Toughness (gf/Denier) | 4.00 |

### 2.5. Admixture

The admixture used is a highly water-reducing super-plasticizer marketed by the Algerian company Granitex under the name 'MEDAPLAST SP 40 in liquid form with a brown color and a PH of 8.2.

### 2.6. Mixing Water

The mixing water used for the preparation of the different mixtures comes from the public drinking water distribution network in compliance with standard NF EN 1008 [29].

### 2.7. Formulation of Sand Concrete

In this study, the formulation approach used is the one defined in the **SABLOCRETE** draft of the revised standard P 18-500 "sand concrete" set out in the book entitled "concretes of sand: characterizations and practice of use" [30]. The composition of different mixtures is summarized in Table 7.

**Table 7.** Formulation of study concretes.

| Denomination of Sand Concretes | Dosage of Constituents in (kg/m$^3$) | | | | | | | |
|---|---|---|---|---|---|---|---|---|
| | Cement CPA | Water | Sand Siliceous (SS) | Sand Quarry (SQ) | Granulated Slag Filler (GS) | P.E.T Fiber | SP | E/C |
| **SSC** | 311.82 | 206.20 | 825.34 | 830.43 | 187 | - | 10 | 0.66 |
| **SC PET 1%** | 311.82 | 206.20 | 820.34 | 825.43 | 187 | 10 | 10 | 0.66 |
| **SC PET 2%** | 311.82 | 206.20 | 815.34 | 820.43 | 187 | 20 | 10 | 0.66 |

<u>Denomination</u> **SSC:** Standard sand concrete. **SC PET 1%:** sand concrete with PET fiber at a rate of 1%. **SC PET 2%:** sand concrete with PET fiber at a rate of 2%.

*2.8. Preparation and Storage of Test Specimens*

The physical–mechanical characteristics of the sand concrete are obtained using measurements of the tensile strength via flexion and compression on specimens that are $4 \times 4 \times 16$ cm$^3$, in accordance with standard NF EN 12390-1 [31]. The preparation of the specimens is carried out according to standard NF EN 12390-2 [32], and the mixing is carried out using a concrete mixer with a capacity of 25 L and a total mixing time of around 5 min.

Vibration is the most common way to give concrete its maximum compactness and to eliminate as many voids as possible. Compaction is carried out on a vibrating table for a total duration of one minute. The specimens are removed from the mold after 24 h and stored at saturated humidity RH = 100% and at a temperature of $20 \pm 2$ °C until the various tests are due.

## 3. Results and Discussion

*3.1. Heat Treatment Cycle for Sand Concrete*

The heat treatment of the specimens was carried out in a Nabertherm muffle furnace (*P330*) (Figure 3) with a temperature programmer and a maximum temperature of 3000 °C. The specimens were subjected to different temperatures (100 °C, 300 °C, 500 °C and 700 °C); a one-hour stability period was applied to homogenize the temperature within the specimens, followed by cooling to room temperature.



**Figure 3.** Muffle furnace.

The heating rate is a factor that has a great influence on the thermal stability of the concrete. The higher the heating rate, the higher the risk of splitting. The characterization tests carried out by [33] on concrete specimens subjected to heating–cooling cycles at a rate of $1\,°C\cdot min^{-1}$ lead to specimen bursting, whereas those subjected to a heating rate of $0.1\,°C\cdot min^{-1}$ do not burst. The low temperature rise rate limits the formation of the saturated zone and reduces the temperature gradient. The rapid heating of the concrete surface generates high thermal gradients (thermal stresses). The thermal gradient generates compressive and tensile stresses that can lead to spalling of the concrete.

*3.2. Properties in the Hardened State*

3.2.1. Physical Properties

Residual Mass Loss

For the determination of the evolution of mass loss as a function of the heating–cooling cycle, the specimens are weighed before and after each heating–cooling cycle [34,35].

The test therefore consists of determining the loss of material that the specimens underwent during heating compared with their initial state (state before heating). The loss of mass expressed as a percentage is obtained as follows:

$$\text{Mass loss} = \frac{M_0 - M_t}{M_0} \times 100(\%) \tag{1}$$

where

$M_0$ is the mass of the test specimen at room temperature (before heating);

$M_t$ is the mass of the cooled specimen after the heating–cooling cycle.

The specimens used are prismatic in shape and have dimensions of $4 \times 4 \times 16\ cm^3$. They are weighed using an electronic balance with an accuracy of 0.1 g.

Figure 4 shows the mass loss of sand concretes with PET fibers in function of the heating temperature.

It can be observed that the increase in temperature leads to a continuous decrease in mass for all concretes. The shape of the mass loss curve is the same for all concretes.

At the temperature of 100 °C, the mass loss is almost identical in all concretes; at this temperature the mass loss was very low. This can be explained by the departure of the free water contained in the pores of the concrete (drying of the concrete).

Afterwards, a strong increase in mass loss is observed. This strong loss of mass is due to the departure of the water initially contained in the hydrates (C-S-H) and to the decomposition of the gypsum ($CaSO_4 2H_2O$) [36].

In the last phase, where the temperature ranges from 300 °C to 700 °C, the loss of mass is due to dehydroxylation of the portlandite. The results found are in agreement with those found in the literature [37–39].

From Figure 4, it can be seen that the addition of the fibers does not change the shape of the mass loss curve. The loss of mass may be related to the melting of the fibers during the temperature rise. These results are in agreement with those found by Zeb B [40]. These mass losses are significant from 0 to 100 °C (loss of 50%) beyond this temperature; mass drops of around 20 to 25% are observed until a temperature of 700 °C is reached.

3.2.2. Mechanical Properties

Residual Compressive Strength

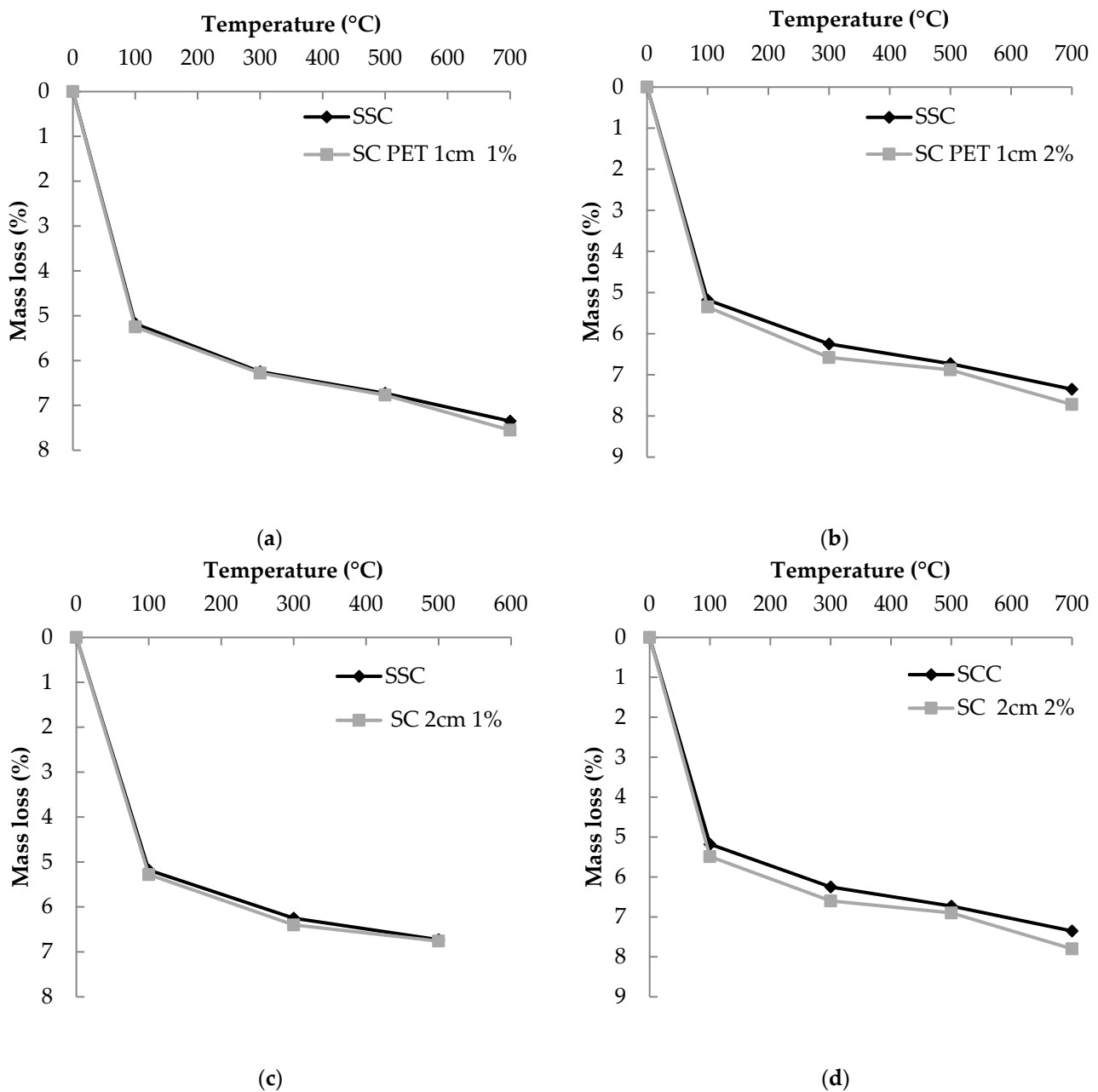Figure 5 shows the evolution of the residual compressive strength in function of the temperature.

(**a**)

(**b**)

(**c**)

(**d**)

**Figure 4.** Loss of mass of sand concrete in function of the heating temperature: (**a**) standard sand concrete and sand concrete with 1 cm 1% of PET, (**b**) standard sand concrete and sand concrete with 1 cm 2% of PET, (**c**) standard sand concrete and sand concrete with 2 cm 1% of PET, and (**d**) standard sand concrete and sand concrete with 2 cm 2% of PET.

Compressive strength is one of the most important properties to characterize a concrete. It decreases overall with increasing temperature [41]. From Figure 5, it can be seen that, as temperature increases, the compressive strength of sand concrete decreases.

At 100 °C, the strengths of sand concrete decrease. The grain size, shape and surface condition of the aggregates can play a secondary role on the mechanical strength of the concrete after the W/C ratio, which is the first-order factor that can influence the latter. The use of a granulated slag filler plays a role in improving the mechanical performance of sand concretes. This is due to the pozzolanic nature of granulated slag fillers, which participate in the formation of secondary hydrates and thus improve the adhesiveness of the aggregates to the cement matrix and to the morphological nature of the sands used (surface condition and porosity) [41,42].
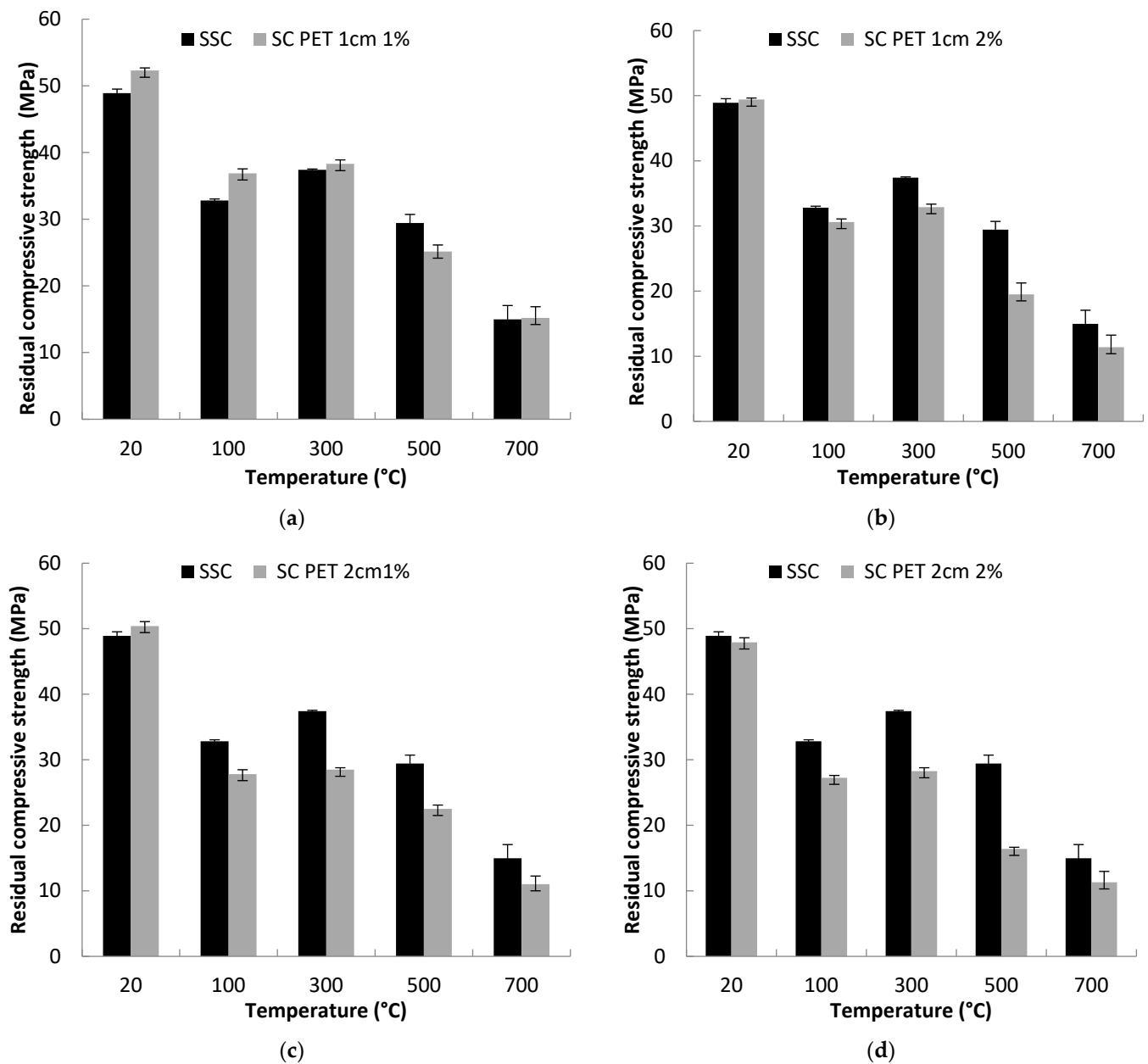
**Figure 5.** Residual compressive strength of sand concrete in function of the heating temperature: (**a**) standard sand concrete and sand concrete with 1 cm 1% of PET, (**b**) standard sand concrete and sand concrete with 1 cm 2% of PET, (**c**) standard sand concrete and sand concrete with 2 cm 1% of PET, and (**d**) standard sand concrete and sand concrete with 2 cm 2% of PET.

Between 20 °C and 100 °C, the resistances of the two types of sand concrete decrease. This is due to the thermal expansion of the water that causes the sheets of the CSH gel to separate. This spacing leads to a reduction in the forces of attraction between the layers and generates the birth of microstructures, causing a reduction in the resistance of the sand concretes.

At 300 °C, a gain in resistance was observed. This gain is due to the departure of the water (the liquid water becomes water vapor and manages to escape from the concrete) allowing a re-increase in the forces of attraction by bringing together the sheets of CSH [43,44].

Above 300 °C, the residual compressive strength decreases more rapidly. The compressive strength obtained after heating to 700 °C is all below 40 MPa. This strong drop in resistance supposes that there was damage to the material. This damage is due to the

degradation of the cementitious matrix and to the disintegration of the aggregates [45]. The second range, above 300 °C, shows a significant decrease in resistance.

The addition of PET fibers does not improve the residual compressive strength. This is due to the increase in porosity with the appearance of micro-cracks, which results in a loss of strength of the concrete. The results obtained are in agreement with those of Valente M et al. [8].

Residual Tensile Strength in Bending

Figure 6 shows the evolution of the residual tensile flexural strength of the concrete in function of the fiber content and the heating temperature.
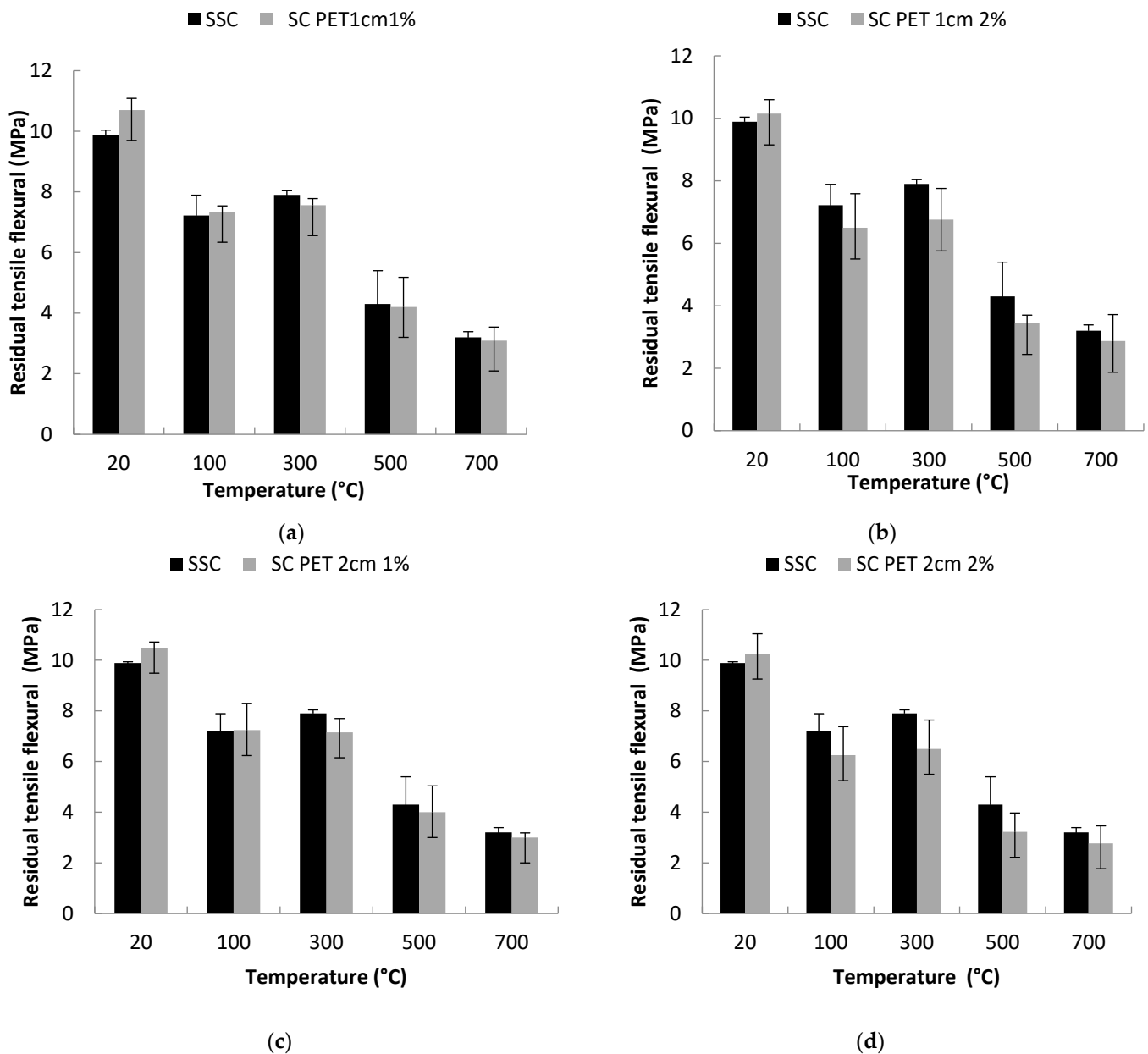


**Figure 6.** Residual tensile flexural strength of sand concrete in function of fiber content and heating temperature: (**a**) standard sand concrete and sand concrete with 1 cm 1% of PET, (**b**) standard sand concrete and sand concrete with 1 cm 2% of PET, (**c**) standard sand concrete and sand concrete with 2 cm 1% of PET, and (**d**) standard sand concrete and sand concrete with 2 cm 2% of PET.

According to Figure 6, the values of the flexural tensile strength of the concretes tested decrease continuously with the rise in temperature. The general appearance of the curve is not modified by the addition of PET fibers, and it is similar to concretes without fibers.

At ambient temperature, sand concrete with PET 1 cm 1% has better tensile strength during bending than concretes without fibers since PET fibers are used in concrete to limit the development of cracking and to prevent the appearance of macrocracks [15].

Above 300 °C, it is observed that the decrease in tensile strength becomes higher. This is due to the degradation of the cementitious matrix (the decomposition of portlandite and CSH). The shape of the curve does not change with the presence of the fibers.

At a temperature of 700 °C, the residual tensile strengths of the concrete with and without fibers are almost the same. We note a total absence of the fibers, which must have completely escaped from the material [11].

The addition of PET fibers in the sand concrete matrix for different rates and different lengths has been studied: an increase in residual stresses is observed at 300 °C. These results are in agreement with those found by Zeb B [40].

### 3.2.3. Optical Photo of the Study Sand Concretes

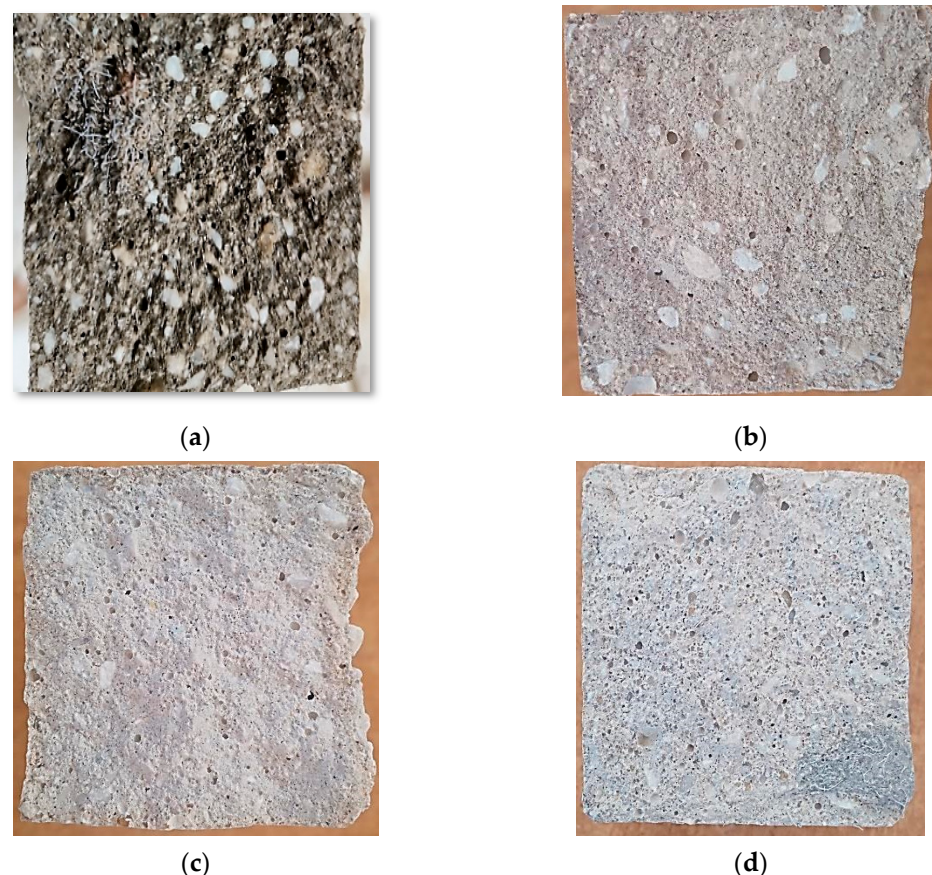Figure 7 presents the optical images of the sand concrete after exposure to different temperatures.



**Figure 7.** Optical picture of sand concrete subjected to different temperatures: (**a**) 100 °C, (**b**) 300 °C, (**c**) 500 °C and (**d**) 700 °C.

Figure 7 clearly shows the total absence of fibers, which must have completely escaped from the material at 100 °C, 300 °C, 500 °C and 700 °C.

The increase in heating temperature affects the PET fibers (calcination); this results in their absence within the matrix and the creation of pores or voids that affect and influence the final structure of the composite and affect its intrinsic properties [12].

### 3.2.4. Morphology of Sand Concretes

Scanning Electron Microscope (SEM) observations for the two types of concrete, namely control sand concrete and sand concrete with 1 cm 1% PET fiber heated to different temperatures (100 °C, 300 °C, 500 °C and 700 °C), are given in Figures 8 and 9. The observations were made on the surface or inside the samples of sand concrete.
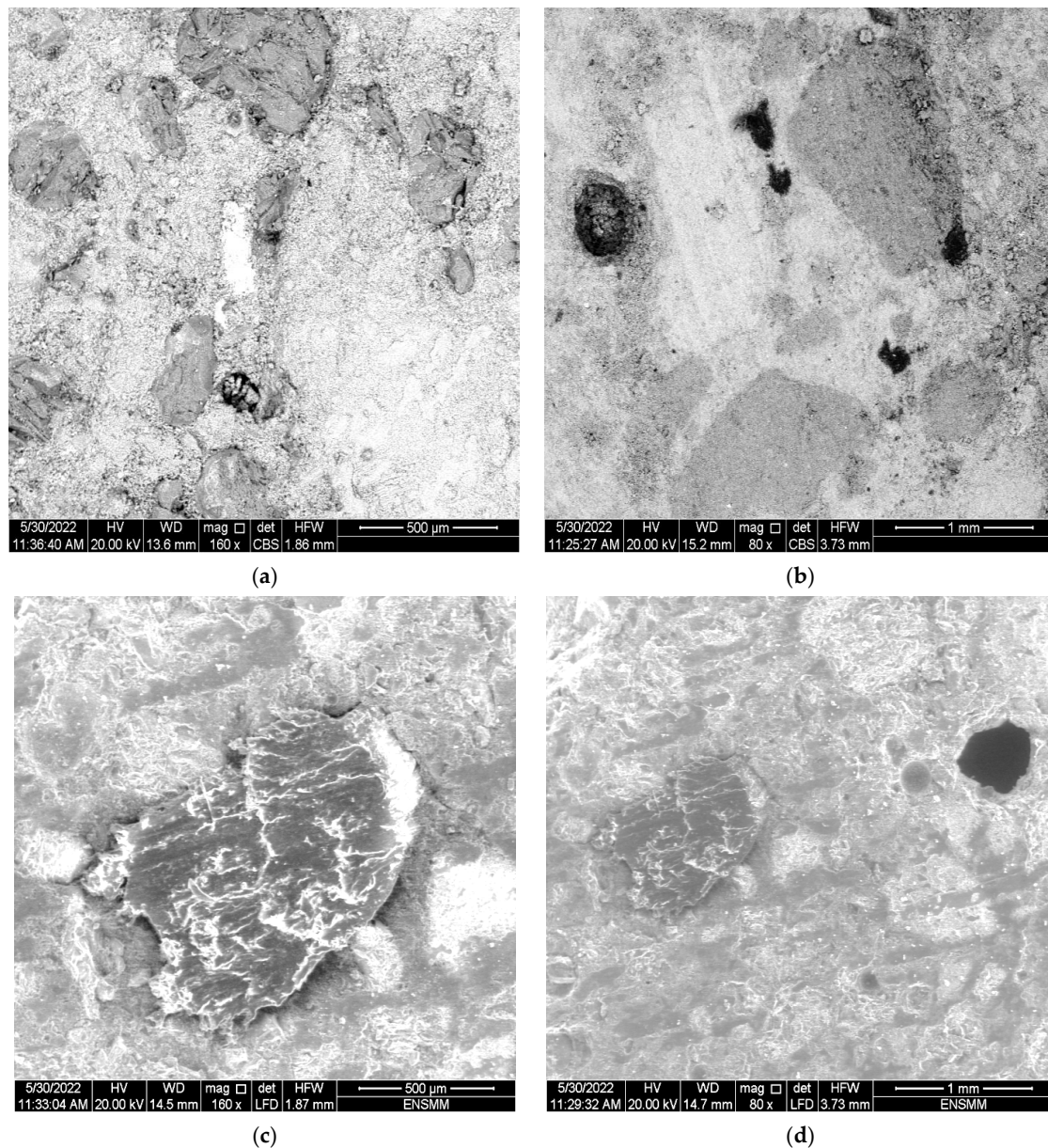


(**a**)

(**b**)

(**c**)

(**d**)

**Figure 8.** Microstructure of standard sand concrete after heating at (**a**) 100 °C, (**b**) 300 °C, (**c**) 500 °C and (**d**) 700 °C.

Figure 8 shows the matrix–aggregate interface areas, compactness and micro-porosity of the control sand concrete. The figure shows that all sand concretes have a dense microstructure with a good cementitious–aggregate matrix bond. On the other hand, after heating to 700 °C, the concrete becomes more porous; this is due to the departure of a large part of the water chemically linked to a high heating temperature [14,15].

Figure 9 shows the presence of a number of visible micro-pores; the number of these pores increases with increasing temperature. The appearance of pores in the sand concrete matrix is due to the evaporation of PET fibers, which resulted in the formation of voids and pores in the cementitious matrix.
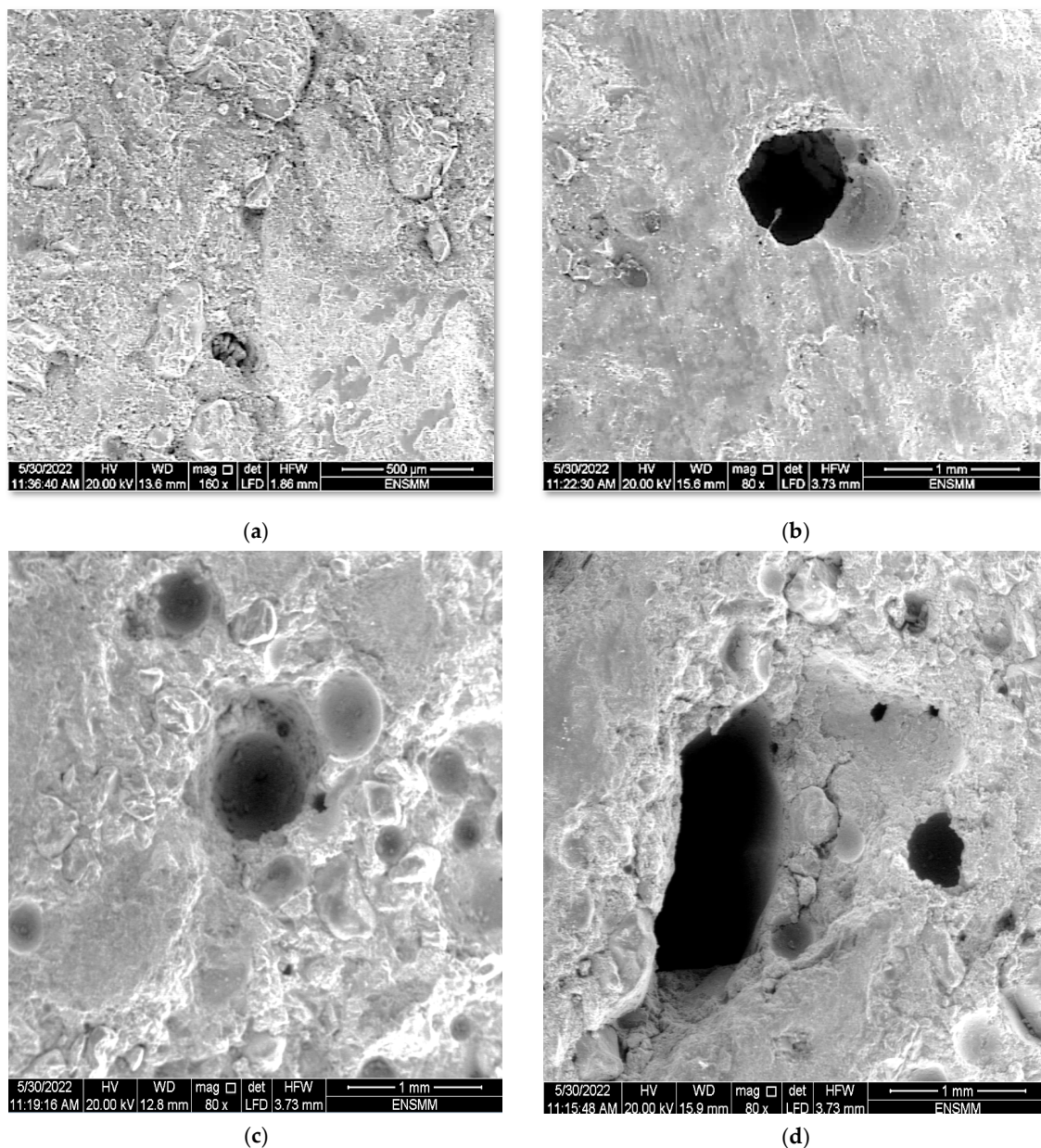
**Figure 9.** Microstructure of standard sand concrete after heating at (**a**) 100 °C, (**b**) 300 °C, (**c**) 500 °C and (**d**) 700 °C.

The SEM observations performed on the heated sand concrete samples confirm the visual observations where the voids increase with increasing heating temperature. Melting these fibers leaves beds of voids, which form a porous network, which can generate stresses and consequently the formation of microcracks [11].

### 3.3. Failure Mode of the Specimens at Different Temperatures

Figure 10 shows the behavior of the standard and PET fiber sand concretes before exposure to high temperatures. It shows the three-point bending test with a 45° mode of failure, which is a common mode in cementitious composites. According to EN 12390-3 [46], this mode is conditioned by the frictional forces that develop between the press plates and the faces of the specimen; these frictional forces are directed towards the interior of the specimen and slow down the evolution of the transverse deformations of the concrete [2,8].

**Figure 10.** The mode of failure of sand concrete before exposure to high temperatures.

Figure 11 shows the behavior of sand concrete with PET fiber exposed at different temperatures. It can be seen that the material presents a quasi-fragile fracture due to the presence of a mainly micro-cracked fracture development zone and size: it develops in front of the crack front. From the point of view of the physical mechanisms characterizing the failure of the concrete, it can be said that it is a brittle, heterogeneous, porous and out-of-equilibrium material by extension. By increasing the applied loads, cracks at 45° are created at the level of the two support zones, resulting from an insufficient resistance of the sand concrete to the shear force [13,18]. Sloping cracks near the supports will suddenly open up and cause the beam to fail. PET fibers can prevent and delay this type of failure, as in the case of reinforced concrete.
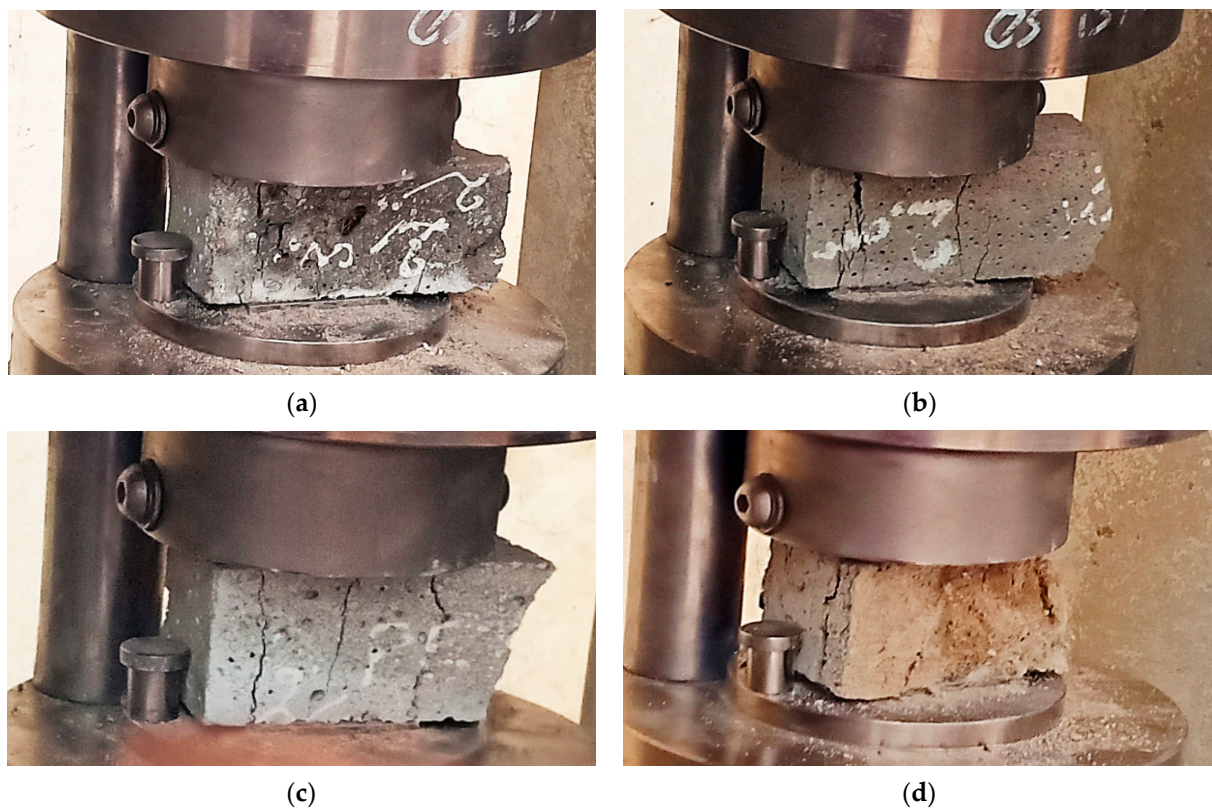


(**a**)

(**b**)

(**c**)

(**d**)

**Figure 11.** The mode of failure of sand concrete exposed to high temperatures: (**a**) 100 °C, (**b**) 300 °C, (**c**) 500 °C and (**d**) 700 °C.

## 4. Conclusions

This study focuses on the development and characterization of sand concrete reinforced with PET fibers subjected to high temperature (100, 300, 500 and 700 °C) by incorporating fibers with different dosage (1% and 2%). Based on the results obtained, we can draw the following conclusions:

- The loss of mass is reduced with the increase in temperature in all concretes.
- The addition of PET fibers shows a slight increase in mass loss compared with that of sand concretes without fibers.
- The studies concretes show a slight decrease in residual compressive strength between ambient temperature and 100 °C.
- The compressive resistance obtained after heating to a temperature of 700 °C are all lower than 40 MPa. This damage is due to the degradation of the cementitious matrix.
- From ambient temperature to 300 °C, a slight improvement in the residual compressive strength of sand concretes with PET fiber was noticed, and above 300 °C, the residual compressive strength drops considerably.
- The addition of PET fibers does not improve the residual compressive strength.
- The residual tensile strength decreases with the rise in temperature for all the sand concretes studied. Beyond 300 °C, the drop in tensile strength becomes higher.
- At ambient temperature, a slight drop in residual tensile strength is noticed for all sand concretes with PET fibers. This may explain why the high dosage of PET fiber (2%) disrupts the crystal lattice of the cementitious matrix.
- The evolution of temperature decreases the residual tensile strength of sand concretes with PET fiber.
- SEM observations show that, at ambient temperature, the sand concrete has a more or less dense microstructure with a minimum of porosity. At 700 °C, the concrete becomes more porous; this can results in melting of the PET fibers during the rise in temperature and the departure of a large part of the water chemically linked to a high heating temperature.
- The addition of PET fibers is generally an effective solution, making it possible to reduce the sensitivity to spalling of the test concretes, to prevent cracking and to fulfill a similar role to that of polypropylene fibers.
- Besides the economic and environmental advantages of the recovery of PET fibers and their use in the reinforcement of innovative concretes, these fibers can help extend the durability concrete and reduce long-term maintenance costs despite the reduction in the mechanical characteristics of concrete and can remain acceptable according to construction standards.

# References

1. Kebaili, B.; Benzerara, M.; Menadi, S.; Kouider, N.; Belouettar, R. Effect of Parent Concrete Strength on Recycled Concrete Performance. *Frattura ed Integrità Strutturale* **2022**, *16*, 14–25. [CrossRef]
2. Rasheed, L.S.; Shaban, A.M.; Abdulrasool, A.T. Mechanical and Structural Characteristics of PET Fiber Reinforced Concrete Plates. *Smart Sci.* **2022**, *10*, 198–212. [CrossRef]
3. Rohman, R.K.; Aji, S. Effect of Fly Ash on Compressive Strength of Concrete Containing Recycled Coarse Aggregate. In *AIP Conference Proceedings, Proceedings of the International Conference on Science and Applied Science (ICSAS) 2018, Surakarta, Indonesia, 12 May 2018*; AIP Publishing LLC: Melville, NY, USA, 2018; Volume 2014, p. 020097.
4. Caporale, A.; Feo, L.; Luciano, R. Limit Analysis of FRP Strengthened Masonry Arches via Nonlinear and Linear Programming. *Compos. Part B Eng.* **2012**, *43*, 439–446. [CrossRef]
5. Ma, Q.; Guo, R.; Zhao, Z.; Lin, Z.; He, K. Mechanical Properties of Concrete at High Temperature: A Review. *Constr. Build. Mater.* **2015**, *93*, 371–383. [CrossRef]
6. Ahn, Y.; Jang, J.G.; Lee, H.-K. Mechanical Properties of Lightweight Concrete Made with Coal Ashes after Exposure to Elevated Temperatures. *Cem. Concr. Compos.* **2016**, *72*, 27–38. [CrossRef]
7. Handoo, S.; Agarwal, S.; Agarwal, S. Physicochemical, Mineralogical, and Morphological Characteristics of Concrete Exposed to Elevated Temperatures. *Cem. Concr. Res.* **2002**, *32*, 1009–1018. [CrossRef]
8. Valente, M.; Sambucci, M.; Sibai, A. Geopolymers vs. Cement Matrix Materials: How Nanofiller Can Help a Sustainability Approach for Smart Construction Applications—A Review. *Nanomaterials* **2021**, *11*, 2007. [CrossRef] [PubMed]
9. Huismann, S.; Weise, F.; Meng, B.; Schneider, U. Transient Strain of High Strength Concrete at Elevated Temperatures and the Impact of Polypropylene Fibers. *Mater. Struct.* **2012**, *45*, 793–801. [CrossRef]
10. Shariq, M.; Soltanzadeh, F.; Masood, A.; Baqi, A. Tensile Strength of Normal and High Strength Concrete with Polypropylene Fibres at Elevated Temperature. In Proceedings of the International Conference on Advances in Civil, Structural and Environmental Engineering, Zurich, Switzerland, 12–13 October 2013; Institute of Research Engineers and Doctors: New York, NY, USA, 2013.
11. Bošnjak, J.; Sharma, A.; Grauf, K. Mechanical Properties of Concrete with Steel and Polypropylene Fibres at Elevated Temperatures. *Fibers* **2019**, *7*, 9. [CrossRef]
12. Mubarak, M.; Muhammad Rashid, R.S.; Amran, M.; Fediuk, R.; Vatin, N.; Klyuev, S. Mechanical Properties of High-Performance Hybrid Fibre-Reinforced Concrete at Elevated Temperatures. *Sustainability* **2021**, *13*, 13392. [CrossRef]
13. Ahmed, W.; Lim, C.W.; Akbar, A. Influence of Elevated Temperatures on the Mechanical Performance of Sustainable-Fiber-Reinforced Recycled Aggregate Concrete: A Review. *Buildings* **2022**, *12*, 487. [CrossRef]
14. Tawfik, M.; El-said, A.; Deifalla, A.; Awad, A. Mechanical Properties of Hybrid Steel-Polypropylene Fiber Reinforced High Strength Concrete Exposed to Various Temperatures. *Fibers* **2022**, *10*, 53. [CrossRef]
15. Al-Ameri, R.A.; Abid, S.R.; Özakça, M. Mechanical and Impact Properties of Engineered Cementitious Composites Reinforced with PP Fibers at Elevated Temperatures. *Fire* **2021**, *5*, 3. [CrossRef]
16. Abdi Moghadam, M.; Izadifard, R. Evaluation of Shear Strength of Plain and Steel Fibrous Concrete at High Temperatures. *Constr. Build. Mater.* **2019**, *215*, 207–216. [CrossRef]
17. Shaikh, F.U.A. Effect of Cooling on the Residual Mechanical Properties and Cracking of Plain and Fibrous Geopolymer Concretes at Elevated Temperatures. *Struct. Concr.* **2019**, *20*, 1583–1595. [CrossRef]
18. Bezerra, A.C.S.; Maciel, P.S.; Corrêa, E.C.S.; Soares Junior, P.R.R.; Aguilar, M.T.P.; Cetlin, P.R. Effect of High Temperature on the Mechanical Properties of Steel Fiber-Reinforced Concrete. *Fibers* **2019**, *7*, 100. [CrossRef]
19. Marzouk, O.Y.; Dheilly, R.; Queneudec, M. Valorization of Post-Consumer Waste Plastic in Cementitious Concrete Composites. *Waste Manag.* **2007**, *27*, 310–318. [CrossRef]
20. Kim, S.B.; Yi, N.H.; Kim, H.Y.; Kim, J.-H.J.; Song, Y.-C. Material and Structural Performance Evaluation of Recycled PET Fiber Reinforced Concrete. *Cem. Concr. Compos.* **2010**, *32*, 232–240. [CrossRef]
21. Foti, D. Preliminary Analysis of Concrete Reinforced with Waste Bottles PET Fibers. *Constr. Build. Mater.* **2011**, *25*, 1906–1915. [CrossRef]
22. Bui, N.K.; Satomi, T.; Takahashi, H. Recycling Woven Plastic Sack Waste and PET Bottle Waste as Fiber in Recycled Aggregate Concrete: An Experimental Study. *Waste Manag.* **2018**, *78*, 79–93. [CrossRef]
23. Al-Hadithi, A.I.; Hilal, N.N. The Possibility of Enhancing Some Properties of Self-Compacting Concrete by Adding Waste Plastic Fibers. *J. Build. Eng.* **2016**, *8*, 20–28. [CrossRef]
24. Passuello, A.; Moriconi, G.; Shah, S.P. Cracking Behavior of Concrete with Shrinkage Reducing Admixtures and PVA Fibers. *Cem. Concr. Compos.* **2009**, *31*, 699–704. [CrossRef]
25. Mohammadhosseini, H.; Yatim, J.M. Microstructure and Residual Properties of Green Concrete Composites Incorporating Waste Carpet Fibers and Palm Oil Fuel Ash at Elevated Temperatures. *J. Clean. Prod.* **2017**, *144*, 8–21. [CrossRef]
26. *NF EN 197-1*; Composition, Specifications and Conformity Criteria for Common Cements. AFNOR: Paris, France, 2012.
27. *BS EN 15167-1*; Ground Granulated Blast Furnace Slag for Use in Concrete, Mortar and Grout. Definitions, Specifications and Conformity Criteria. European Standard: Pilsen, Czech Republic, 2006.
28. MediFil, F. Product Leaflet MediFil Polyethylene Terephthalate, PET. In *Fiber Data Sheet*; Setif, Algeria, 2022.
29. *NF EN 1008*; Eau Gâchage Pour Bétons-Spécifications Déchantillonnage Essais Dévaluation Aptit. À Empl. Compris Eaux Process. Ind. Béton Telle Que Eau Gâchage Pour Béton Indice Classem. AFNOR: Paris, France, 2003; pp. 18–211.

30. Sablocrete. *Bétons de Sable: Caractéristiques et Pratiques d'utilisation*; Projet National de Recherche/Développement; Presses de l'Ecole Nationale des Ponts et Chaussées: Paris, France, 1994; ISBN 2-85978-221-4.

31. *NF EN 12390-1*; Essai Pour Béton Durci-Partie 1 Forme Dimens. Autres Éxigences Relat. Aux Éprouvettes Aux Moules. AFNOR: Paris, France, 2001.

32. *NF EN 12390-2*; Essais Pour Béton Durci-Partie 2 Confect. Conserv. Éprouvettes Pour Essais Résistance. AFNOR: Paris, France, 2001.

33. Haddad, R.H.; Al-Saleh, R.J.; Al-Akhras, N.M. Effect of Elevated Temperature on Bond between Steel Reinforcement and Fiber Reinforced Concrete. *Fire Saf. J.* **2008**, *43*, 334–343. [CrossRef]

34. Pliya, P.; Beaucour, A.; Noumowé, A. Contribution of Cocktail of Polypropylene and Steel Fibres in Improving the Behaviour of High Strength Concrete Subjected to High Temperature. *Constr. Build. Mater.* **2011**, *25*, 1926–1934. [CrossRef]

35. Xiao, J.; Falkner, H. On Residual Strength of High-Performance Concrete with and without Polypropylene Fibres at Elevated Temperatures. *Fire Saf. J.* **2006**, *41*, 115–121. [CrossRef]

36. Noumowé, N. Effet de Hautes Températures Sur Le Béton (20-600 C), Cas Particulier Du Béton à Hautes Performances. Ph.D. Thesis, INSA de Lyon, Villeurbanne, France, 1995.

37. Harmathy, T.Z. Moisture in Materials in Relation to Fire Test. *ASTM Spec. Tech. Publ.* **1964**, *385*, 74–95.

38. Hertz, K.D. Limits of Spalling of Fire-Exposed Concrete. *Fire Saf. J.* **2003**, *38*, 103–116. [CrossRef]

39. Noumowe, A.N. Temperature Distribution and Mechanical Properties of High-Strength Silica Fume Concrete at Temperatures up to 200 °C. *Mater. J.* **2003**, *100*, 326–330.

40. Zeb, B. *The Effect of High Temperature on Concrete Containing Fibers from Recycled Plastic Bottles*; Universiti Teknologi: Skudai, Malaysia, 2017.

41. Siddique, R.; Kaur, D. Properties of Concrete Containing Ground Granulated Blast Furnace Slag (GGBFS) at Elevated Temperatures. *J. Adv. Res.* **2012**, *3*, 45–51. [CrossRef]

42. Gong, W.; Chen, Q.; Miao, J. Bond Behaviors between Copper Slag Concrete and Corroded Steel Bar after Exposure to High Temperature. *J. Build. Eng.* **2021**, *44*, 103312. [CrossRef]

43. Phan, L.T.; Carino, N.J. Code Provisions for High Strength Concrete Strength-Temperature Relationship at Elevated Temperatures. *Mater. Struct.* **2003**, *36*, 91–98. [CrossRef]

44. Castillo, C. *Effect of Transient High Temperature on High-Strength Concrete*; Rice University: Houston, TX, USA, 1987.

45. Hager, I. Comportement à Haute Température Des Bétons à Haute Performance: Évolution Des Principales Propriétés Mécaniques. Ph.D. Thesis, ENPC, Marne-la-Vallée, France, 2004.

46. *NF EN 12390-3*; Essai Pour Béton Durci Partie 3 Résistance À Compression Sur Éprouvette. AFNOR: Paris, France, 2000.